Implementation of fundamental-solution based hybrid finite element model for elastic circular inclusions

H. Wang[1] and Qing H. Qin[2,*]

[1]Department of Mechanics, Henan University of Technology, Zhengzhou 450001, China
[2]Research School of Engineering, Australian National University, ACT 0200, Australia

*Corresponding author: qinghua.qin@anu.edu.au

Abstract

In this paper, a doubly periodic array of inclusions in infinite plane matrix is studied for analyzing its effective elastic properties. A representative rectangular cell containing single inclusion is taken from the composites and then is investigated using the present hybrid finite element model to obtain numerical results of boundary tractions under the applied displacement boundary conditions. In the present numerical model, a general polygonal hybrid finite element with arbitrary number of sides is constructed by coupling the independent element interior and frame displacement fields. The element interior fields are approximated by the combination of fundamental solutions to prior satisfy the governing equation of the problem, so that the domain integral appeared in the weak-form functional is converted into boundary integrals. Independently the element frame fields are approximated by the conventional shape functions to guarantee the continuity conditions across inter-element boundaries. Following this, the polygonal inclusion elements are designed to reduce mesh effort in the inclusion domain. Numerical tests are conducted for assessing the performance of the element model and it is found that the present method gives good accuracy as compared with the conventional finite element.

Keywords: Representative volume element; Effective elastic properties; Fundamental solutions; Polygonal inclusion element.

Introduction

In the context of composite with reinforced inclusions, the simplified model with periodic distribution of multiple inclusions is usually taken as an example for determining the corresponding effective properties of composites. However, the analytical methods (Yu and Qin, 1996; Feng et al., 2003; 2004; Bonnet, 2007; Nemat-Nasser and Hori, 1999; Qin and Yang, 2009; To et al, 2013) like fast Fourier transforms and so on are usually difficult to deal with composites containing the inclusion with complicated geometric shapes or distributions. As alternatives to the analytical methods, numerical methods were developed for solving composite problems involving various periodic inclusions (Dong, 2006; Kaminski, 1999; Michel et al., 1999; Qin, 2004; Yang and Qin, 2003; 2004; Wang and Qin, 2011a; Würkner et al., 2011). For example, Würkner et al. (2011) evaluated the effective material properties for composite structures with rhombic fiber arrangements by the finite element method (FEM). Michel et al. (1999) compared the two numerical methods including the finite element method and the fast Fourier transform-based numerical method in determining effective properties of composite materials with periodic microstructure. Yang and Qin (2003) studied the effect of fiber bundling on the effective transverse properties of unidirectional fiber composites by way of finite element method. Dong (2006) employed the boundary element method (BEM) to predict the effective elastic properties of composites including doubly periodic array of inclusions. Yang and Qin (2004) extended the boundary element formulation to the micro-mechanical analysis of composite materials. Kaminski (1999) employed the boundary element method based homogenization to deal with the periodic transversely isotropic linear elastic fiber-reinforced composites. Besides the FEM and the BEM, Wang and Qin (2011a) developed the hybrid finite element formulation for analyzing the effective thermal conductivity of fiber-reinforced composites, in which the fiber can be regularly, or randomly distributed.

Among the numerical methods mentioned above, the hybrid finite element method based on fundamental solutions has shown its advantages over the others (Qin, 2005; Qin and Wang, 2008; Wang and Qin, 2010). One feature of the method is the use of special elements. Within the developed special elements (Wang and Qin, 2011b), special fundamental solutions analytically satisfying the governing equations and certain boundary conditions are employed to approximate the internal displacement and stress fields. Besides the development of special elements based on the special fundamental solutions, another feature of the hybrid model is to construct arbitrarily shaped elements with more nodes and edges, because all integrals appearing in the hybrid model are boundary integrals along the element frame.

In the paper, large polygonal elements or super elements with many edges and nodes are developed for solving such problems as composites with doubly periodic circular inclusions, and the corresponding hybrid finite element formulation for calculating effective properties of the composite is presented.

Computational model and effective elastic properties

Consider a composite with doubly periodic inclusions of arbitrary shape in an infinite plane matrix subject to remote tension σ_{11}^{∞}, σ_{22}^{∞} and in-plane shear forces σ_{12}^{∞} (see Fig. 1). The elastic parameters of inclusion and matrix are respectively denoted by $E^{(\mathrm{I})}$ and $v^{(\mathrm{I})}$, and $E^{(\mathrm{M})}$ and $v^{(\mathrm{M})}$.

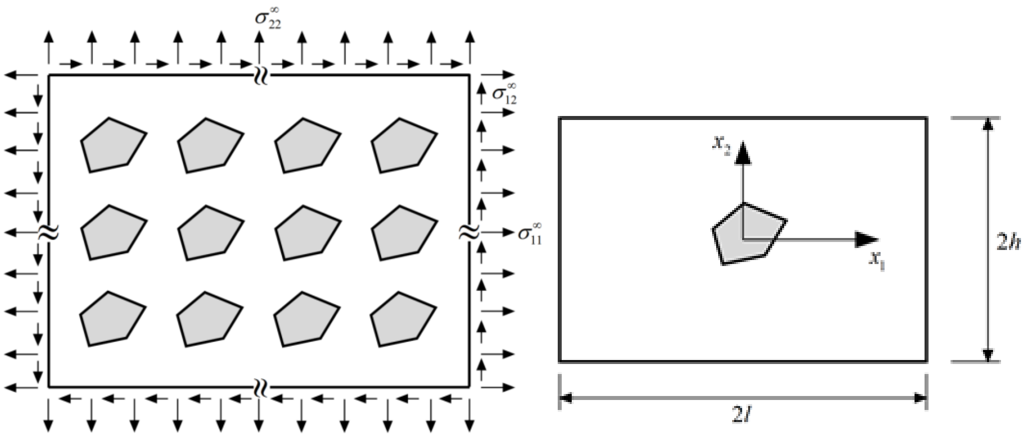

Fig. 1 Sketch of doubly periodic inclusions with arbitrary shape in the infinite plane matrix and a rectangular cell containing single inclusion of arbitrary shape

For such periodic structure, a representative rectangular cell shown in Fig. 1 with edge length $2l$ and $2h$ along the coordinate directions x_1 and x_2 are chosen as an example. On the outer boundary of the cell, the suitable periodic boundary conditions corresponding to remote tension and shear forces, respectively are given by (Dong, 2006).

Because a solid containing doubly periodic array of inclusions with arbitrary shape considered in the paper is usually considered as a homogeneous orthotropic solid, the corresponding constitutive relationship associated to average stresses $\bar{\sigma}_{ij}$ and strains $\bar{\varepsilon}_{ij}$ can be written as (Kaw, 2006; Nemat-Nasser and Hori, 1999)

$$\bar{\varepsilon}_{11} = \bar{\sigma}_{11} / \bar{E}_1 - \bar{v}_{21}\bar{\sigma}_{22} / \bar{E}_2, \quad \bar{\varepsilon}_{22} = \bar{\sigma}_{22} / \bar{E}_2 - \bar{v}_{12}\bar{\sigma}_{11} / \bar{E}_1, \quad \bar{\gamma}_{12} = \bar{\sigma}_{12} / \bar{G}_{12} \tag{1}$$

where $\bar{E}_1$, $\bar{E}_2$, $\bar{v}_{21}$, $\bar{v}_{12}$ and $\bar{G}_{12}$ are effective orthotropic elastic parameters, respectively.

In order to determine the effective elastic properties $\bar{E}_2$ and $\bar{v}_{21}$, the remote loading conditions can be given by

$$\sigma_{11}^{\infty} = 0, \quad \sigma_{22}^{\infty} = p, \quad \sigma_{12}^{\infty} = 0 \tag{2}$$

Thus, in the effective homogeneous orthotropic solid, the average stress and strain states are separately written by

$$\bar{\sigma}_{11}=0,\quad \bar{\sigma}_{22}=p,\quad \bar{\sigma}_{12}=0,\quad \bar{\varepsilon}_{11}=u_{l1}/l,\quad \bar{\varepsilon}_{22}=u_{h2}/h \tag{3}$$

Substituting Eq. (3) into Eq. (1) yields

$$\begin{cases}\bar{\varepsilon}_{11}=-\bar{\nu}_{21}p/\bar{E}_2=u_{l1}/l\\ \bar{\varepsilon}_{22}=p/\bar{E}_2=u_{h2}/h\end{cases}\Rightarrow\begin{cases}\bar{E}_2=ph/u_{h2}\\ \bar{\nu}_{21}=-u_{l1}h/(u_{h2}l)\end{cases} \tag{4}$$

where u_{l1}, u_{l2}, u_{h1} and u_{h2} are the unknown displacements to be determined.

Similarly, in order to determine the effective elastic properties $\bar{E}_1$ and $\bar{\nu}_{12}$, the remote loading conditions can be given by

$$\sigma_{11}^{\infty}=p,\quad \sigma_{22}^{\infty}=0,\quad \sigma_{12}^{\infty}=0 \tag{5}$$

To find the effective shear modulus, one needs to apply the remote shear loading, i.e.

$$\sigma_{11}^{\infty}=0,\quad \sigma_{22}^{\infty}=0,\quad \sigma_{12}^{\infty}=p \tag{6}$$

The corresponding average stress and strain states can be written as

$$\bar{\sigma}_{11}=0,\quad \bar{\sigma}_{22}=0,\quad \bar{\sigma}_{12}=p,\quad \bar{\gamma}_{12}=u_{l2}/h+u_{h1}/l \tag{7}$$

Substituting Eq. (7) into Eq. (1), one obtains

$$\bar{G}_{12}=p/\bar{\gamma}_{12} \tag{8}$$

From the procedure above, it can be seen that for three cases including single tension along the x_1 direction, single tension along the x_2 direction and in-plane shear, the relation of the remote stresses and the displacement boundary conditions should be established to determine the effective properties of the composite. According to the formulations in the literature (Dong, 2006), the traction variation along the outer boundary of the cell taken from the composite must be evaluated under the applied unit displacement boundary conditions, and this procedure can be performed by using the present super element below.

Basic formulations and polygonal inclusion elements

Basic formulations

For the matrix and inclusion under consideration, the integral formulation of hybrid finite element in a particular hybrid element e can be written as follows (Wang and Qin, 2010; Wang and Qin, 2011b)

$$\Pi_{me}=\frac{1}{2}\int_{\Omega_e}\boldsymbol{\sigma}^{\mathrm{T}}\boldsymbol{\varepsilon}\mathrm{d}\Omega-\int_{\Gamma_e^s}\bar{\mathbf{s}}^{\mathrm{T}}\tilde{\mathbf{u}}\mathrm{d}\Gamma+\int_{\Gamma_e}\mathbf{s}^{\mathrm{T}}\left(\tilde{\mathbf{u}}-\mathbf{u}\right)\mathrm{d}\Gamma \tag{9}$$

where $\boldsymbol{\sigma}=\{\sigma_{11}\quad\sigma_{22}\quad\sigma_{12}\}^{\mathrm{T}}$, $\boldsymbol{\varepsilon}=\{\varepsilon_{11}\quad\varepsilon_{22}\quad\gamma_{12}\}^{\mathrm{T}}$ and $\mathbf{u}=\{u_1\quad u_2\}^{\mathrm{T}}$ are respectively stress, strain and displacement fields in the element domain Ω_e, $\tilde{\mathbf{u}}=\{\tilde{u}_1\quad\tilde{u}_2\}^{\mathrm{T}}$ is the compatible displacement field defined on the boundary $\partial\Omega_e=\Gamma_e$ with an outward normal $\mathbf{n}=\{n_1\quad n_2\}^{\mathrm{T}}$, $\mathbf{s}=\mathbf{A}\boldsymbol{\sigma}$ is the traction field and $\bar{\mathbf{s}}$ denotes the specified traction on the boundary Γ_e^s.

Provided that the internal displacement and stress fields satisfy the governing equation in the element domain, applying the Gaussian divergence theorem to the functional Π_{me} yields

$$\Pi_{me}=-\frac{1}{2}\int_{\Gamma_e}\mathbf{u}^{\mathrm{T}}\mathbf{s}\mathrm{d}\Gamma-\int_{\Gamma_e^s}\bar{\mathbf{s}}^{\mathrm{T}}\tilde{\mathbf{u}}\mathrm{d}\Gamma+\int_{\Gamma_e}\mathbf{s}^{\mathrm{T}}\tilde{\mathbf{u}}\mathrm{d}\Gamma \tag{10}$$

In the application of variational principle, the displacement field in the interior of the element is approximated by a linear combination of fundamental solutions centered at series of source points $\mathbf{x}^s$ locating on the pseudo boundary similar to the element boundary Γ_e, that is,

$$\mathbf{u}=\mathbf{N}\mathbf{c}_e \tag{11}$$

Subsequently, according to the strain-displacement equations and the stress-strain relationship, the corresponding stress components and tract components are expressed as

$$\boldsymbol{\sigma} = \mathbf{T}\mathbf{c}_e \quad \text{and} \quad \mathbf{s} = \mathbf{Q}\mathbf{c}_e \tag{12}$$

In order to enforce the conformity of the displacement field on the common interface of adjacent elements, the element boundary displacement field $\tilde{\mathbf{u}}$ can be interpolated from the generalized nodal displacement $\mathbf{d}_e$ in the form

$$\tilde{\mathbf{u}} = \tilde{\mathbf{N}}\mathbf{d}_e \tag{13}$$

where $\tilde{\mathbf{N}}$ denotes the matrix consisting of shape functions widely used in the standard FEM and BEM.

The substitution of Eqs. (11) and (13) into the functional **Error! Reference source not found.** including boundary integrals only gives

$$\Pi_{me} = -\frac{1}{2}\mathbf{c}_e{}^{\mathrm{T}}\mathbf{H}_e\mathbf{c}_e - \mathbf{d}_e{}^{\mathrm{T}}\mathbf{g}_e + \mathbf{c}_e{}^{\mathrm{T}}\mathbf{G}_e\mathbf{d}_e \tag{14}$$

where

$$\mathbf{H}_e = \int_{\Gamma_e} \mathbf{Q}^{\mathrm{T}}\mathbf{N}\mathrm{d}\Gamma, \quad \mathbf{G}_e = \int_{\Gamma_e} \mathbf{Q}^{\mathrm{T}}\tilde{\mathbf{N}}\mathrm{d}\Gamma, \quad \mathbf{g}_e = \int_{\Gamma_e^s} \tilde{\mathbf{N}}^{\mathrm{T}}\bar{\mathbf{s}}\mathrm{d}\Gamma \tag{15}$$

The stationary of Π_{me} with respect to the displacement coefficient $\mathbf{c}_e$ and nodal displacement $\mathbf{d}_e$ yields the following optional relationship between $\mathbf{c}_e$ and $\mathbf{d}_e$

$$\mathbf{c}_e = \mathbf{H}_e^{-1}\mathbf{G}_e\mathbf{d}_e \tag{16}$$

and the element displacement-load equation given by

$$\mathbf{K}_e\mathbf{d}_e = \mathbf{g}_e \tag{17}$$

where $\mathbf{K}_e = \mathbf{G}_e{}^{\mathrm{T}}\mathbf{H}_e^{-1}\mathbf{G}_e$ is the symmetric element stiffness matrix, like the one in the conventional FEM.

Polygonal inclusion elements

It's known that the conventional displacement finite element method with polynomial representations is difficult to construct an element with arbitrary number of sides. However, from the hybrid formulation described above we can see that it is appropriate for constructing *n*-sided polygonal elements more nodes and edges than the conventional finite elements, due to the fact of the independence of interior displacement fields and boundary displacements. More importantly, because the interior approximation displacement and stress fields analytically satisfy the elastic governing equations within the element domain, all integrals are evaluated along the element boundary. Thus, it's possible to design the super elements with multiple element edges to achieve the effort of mesh reduction in the inclusion region.

Although arbitrarily shaped inclusions such as circular, triangular or square inclusions can be studied theoretically using the present hybrid finite element formulation, in the paper, just the circular inclusion is studied for the sake of simplicity. Then, the hybrid super elements with multi-edges shown in Fig. 1 can be used to model the inclusion. In Fig. 1, the solid line represents the inclusion element boundary, while the dash line is the *pseudo* boundary which is similar to the element boundary from the point of geometry. The triangle symbol is the center of the inclusion of interest. Source points are preassigned on the pseudo boundary and can be generated by means of the relation

$$\mathbf{x}^s = \mathbf{x}_c + \gamma\mathbf{x}_b \tag{18}$$

where $\mathbf{x}^s$ and $\mathbf{x}_b$ are respectively the source point and boundary node, and $\mathbf{x}_c$ denotes the element centroid. The dimensionless parameter γ scales the distance of the pseudo boundary and the element boundary (Wang et al, 2005; Wang and Qin, 2008).

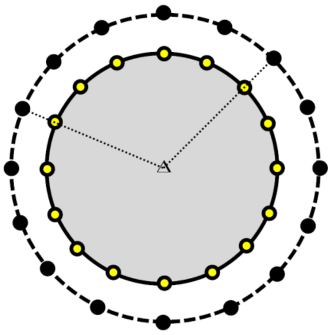

Fig. 1 Configuration of hybrid element with multi-edges for circular inclusion

Numerical examples

The matrix in the composite with doubly period circular inclusions is considered to be isotropic and homogeneous, and the elastic modulus and Poisson's ratio of the medium are respectively taken as E^{M}=1, v^{M}=0.3. The isotropic and homogeneous elastic inclusion is assumed to have same Poisson's ration as that of matrix, and its elastic modulus is assumed to be $E^{\mathrm{I}}/E^{\mathrm{M}}$=10. For the sake of convenience, the geometry size of the RVE is taken as *h/l*=1 with the assumption of $h=0.5$.

In order to investigate the effect of inclusion on the mechanical properties of composites, the effective elastic properties are compared for the circular inclusion under same volume fraction. For example, if the value of volume fraction is supposed to be α, the corresponding geometrical characteristic parameter for the circular inclusion can be determined, i.e. radius of the circular inclusion=$\sqrt{4hl\alpha/\pi}$.

*Inversion of **H** matrix*

From the hybrid finite element formulation given above, one observes that the mechanical properties of the present hybrid element with multiple edges are associated with the inverse operation of matrix **H.** In order to investigate the accuracy of the inverse operation of matrix **H**, the following problem involving the circular inclusion only is firstly considered. The radius of the circle is taken to be unit. The boundary of the circle is discretized by one super element with *k* edges including three nodes each, thus the total number of nodes for the super element is *2k*.

To reveal the ill-conditioning of the matrix **H**, the singular value decomposition is employed herein. Let **H** be a square matrix with *n* by *n* entries. Then the SVD of **H** is a decomposition of the form

$$\mathbf{H} = \mathbf{U}\mathbf{S}\mathbf{V}^T = \sum_{i=1}^{n} \mathbf{u}_i \sigma_i \mathbf{v}_i^T \tag{19}$$

where $\mathbf{U} = (\mathbf{u}_1, \mathbf{u}_2, \cdots, \mathbf{u}_n)$ and $\mathbf{V} = (\mathbf{v}_1, \mathbf{v}_2, \cdots, \mathbf{v}_n)$ are matrices with orthonormal columns, that is, $\mathbf{U}^T\mathbf{U} = \mathbf{V}^T\mathbf{V} = \mathbf{I}$, and $\mathbf{S} = \mathrm{diag}(\sigma_1, \sigma_2, \cdots, \sigma_n)$ has non-negative diagonal elements appearing in non-increasing order such that

$$\sigma_1 \geq \sigma_2 \geq \cdots \geq \sigma_n$$

As a result, the matrix condition number of **H** can be given by the ratio σ_1 / σ_n, and the inverse of **H** is evaluated by

$$\mathbf{H}^{-1} = \mathbf{V}\mathbf{S}^{-1}\mathbf{U}^T \tag{20}$$

In the following test, a super-element with k =8 and 20 edges is considered and the size of **H** matrix is $4k$ by $4k$. To investigate the accuracy of the matrix inversion of H, we evaluate the norm of the residue matrix $\mathbf{HH}^{-1}-\mathbf{I}$ for various values of γ.

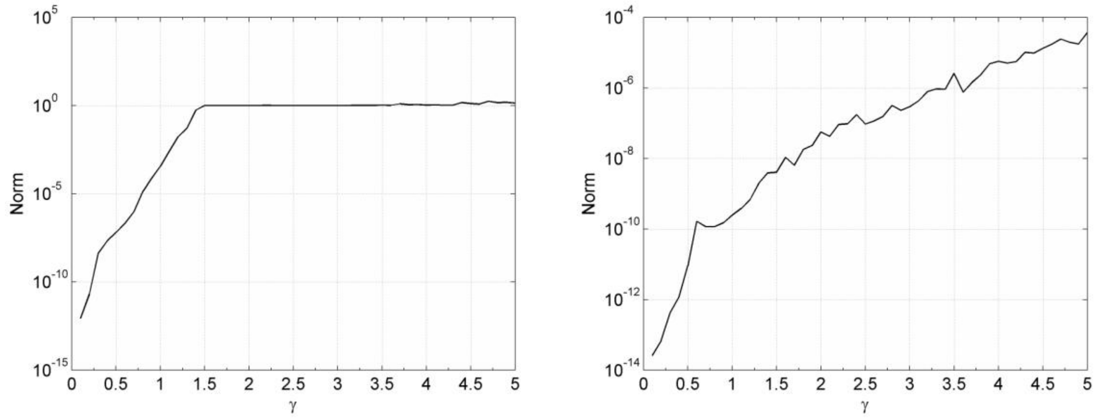

(a) Number of edges k=20 (b) Number of edges k=8

Fig. 3 The norm for various number of element edges

From the numerical results shown in Fig. 3, we can conclude that the total number of element nodes affects the choice of the parameter γ, which is important to keep the inversion of **H** stable and accurate. To establish a proper rule to determine the value of γ according to the specified element type, the maximum value of γ is in proper value when the corresponding norm of inversion is less than 10^{-6}. In Fig. 4, the maximum proper value of γ is plotted as the change of number of degrees of freedom (DOFs) of the element. Subsequently, the curve fitting technology is employed to give an approximated expression of the maximum proper value of γ in terms of number of DOFs of the element, which is denoted by the symbol x. Here, we employ the 6^{th} degree polynomial to perform the curve fitting

$$\gamma = p_1x^6 + p_2x^5 + p_3x^4 + p_4x^3 + p_5x^2 + p_6x + p_7 \tag{21}$$

with

$$p_1 = -2.782\times10^{-10},\ p_2 = 5.274\times10^{-8},\ p_3 = 1.033\times10^{-7}$$
$$p_4 = -7.219\times10^{-4},\ p_5 = 6.869\times10^{-2},\ p_6 = -2.690,\ p_7 = 41.92$$

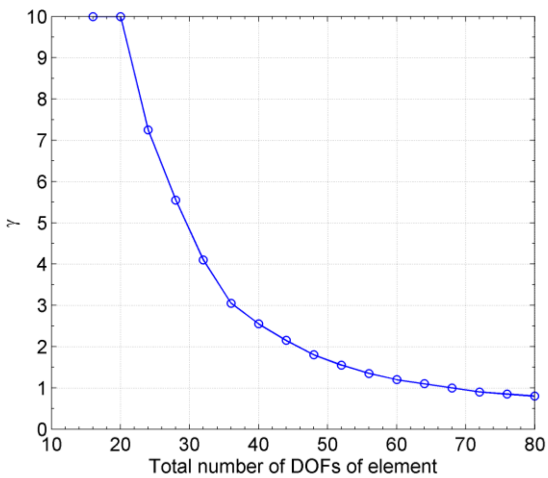

Fig. 4 The maximum proper value of γ for different number of DOFs of the element

Circular inclusion

Next, in this section, the mechanical response of the composite with circular inclusion is taken into considered for the purpose of estimating the effective properties of the composite in the future. For convenience, the RVE is assumed to be subjected to a unit uniform tension along the vertical direction.

For a moderate volume fraction of the inclusion, i.e. α=10%, the typical mesh division is shown in Fig. 5. To make comparison, we keep the mesh same in the matrix for both ABAQUS and HFS-FEM, while in the inclusion, the mesh strategy is different. For the mesh discretization generated by ABAQUS, some typical quadratic isoparametric elements are produced to discretize the inclusion domain. The total number of elements in the ABAQUS is 124 elements with 405 nodes. In contrast, a super element with 20 edges is employed in the developed HFS-FEM to model the inclusion and no any nodes are put inside the inclusion. Thus, the total number of elements in the present HFS-FEM is just 81 elements and the number of nodes reduces to 292. It's clear that the effect on mesh reduction is achieved by the present super hybrid element.

Besides, the variation of traction components along the outer boundary of the RVE is displayed in Fig. 6, from which we observe that there is a good agreement between the numerical results of HFS-FEM and those of ABAQUS. So, the accuracy and efficiency of the present super hybrid element is demonstrated for the analysis of composite embedded with circular inclusions.

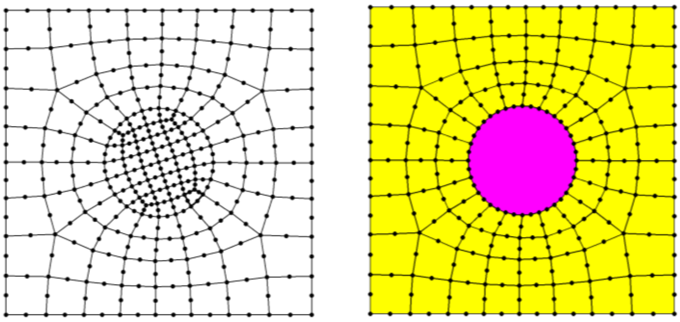

(a) (b)

Fig. 5 Illustration of mesh division in: (a) ABAQUS (b) HFS-FEM for the case of α=10%

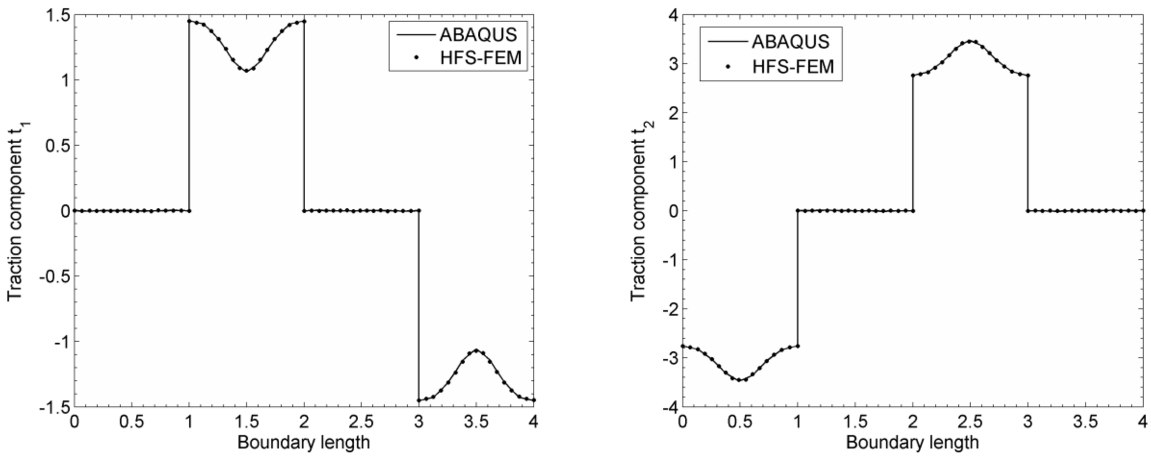

Fig. 6 Traction distribution along the outer boundary of RVE for the case of α=10%

5. Conclusions

The present study proposes a fundamental-solution-based hybrid finite element formulation for the analysis of unidirectional fiber reinforced composites. The fiber is with circular cross section. By virtue of the property of the present hybrid element, we can construct a super inclusion element with multiple edges and nodes for the purpose of mesh reduction and don't need to make any mesh discretization inside the inclusion. The numerical results from the proposed element model are in good agreement with those from ABAQUS, which indicates that the present hybrid finite element is effective and convenient for determining effective properties of composites with doubly periodic array of circular inclusions. In the future, elements for modeling composites containing other shaped inclusions including triangular, square and elliptic inclusions will be studied to investigate the shape effect of the inclusions on the elastic properties of the composite.

Acknowledgements The work described in this paper was partially supported by the National Natural Science Foundation of China (No. 11102059), and the Program for Innovation Talents of Science and Technology in Universities in Henan Province (No. 13HASTIT019).

References

Bonnet G. (2007), Effective properties of elastic periodic composite media with fibers. *J Mech Phys Solids*, 55, pp. 881-899.

Dong, C.Y. (2006), Effective elastic properties of doubly periodic array of inclusions of various shapes by the boundary element method. *Int J Solid Struct*, 43, pp. 7919-7938.

Feng, X.Q., Mai, Y.W. and Qin, Q.H. (2003), A micromechanical model for interpenetrating multiphase composites. *Comput Mater Sci*, 28, pp. 486-493.

Feng, X.Q., Qin, Q.H. and Yu, S.W. (2004), Quasi-micromechanical damage model for brittle solids with interacting microcracks. *Mech Mater*, 36, pp. 261-273.

Kaminski M. (1999), Boundary element method homogenization of the periodic linear elastic fiber composites. *Eng Anal Bound Elem*, 23, pp. 815-824.

Kaw A.K. (2006), *Mechanics of Composite Materials*. CRC Press.

Michel J., Moulinec H., Suquet P. (1999), Effective properties of composite materials with periodic microstructure: a computational approach. *Comput Method Appl M*, 172, pp. 109-143.

Nemat-Nasser, S. and Hori, M. (1999), *Micromechanics: Overall properties of heterogeneous materials*. Elsevier.

Qin, Q.H. (2004), Micromechanics-BE solution for properties of piezoelectric materials with defects. *Eng Anal Bound Elem*, 28, pp. 809-814.

Qin, Q.H. (2005), Trefftz finite element method and its applications. *Appl Mech Reviews*, 58, pp.316-337.

Qin, Q.H. and Wang, H. (2008), *Matlab and C programming for Trefftz finite element methods*. CRC Press.

Qin, Q.H. and Yang, Q.S. (2009), *Macro-micro theory on multifield coupling behavior of heterogeneous materials*. Higher Education Press and Springer.

To, Q.D., Bonnet G., To V.T. (2013), Closed-form solutions for the effective conductivity of two-phase periodic composites with spherical inclusions. *P Roy Soc A-Math Phy*, 469, pp. 20120339

Wang, H. and Qin, Q.H. (2008), Meshless approach for thermo-mechanical analysis of functionally graded materials. *Eng Anal Bound Elem*, 32, pp. 704-712.

Wang, H. and Qin, Q.H. (2010), Fundamental-solution-based finite element model for plane orthotropic elastic bodies. *Eur J Mech A-Solid*, 29, pp. 801-809.

Wang, H. and Qin QH. (2011a), Special fiber elements for thermal analysis of fiber-reinforced composites. *Eng Comput*, 28, pp. 1079-1097.

Wang, H. and Qin, Q.H.(2011b), Fundamental-solution-based hybrid FEM for plane elasticity with special elements. *Comput Mech*, 48, pp. 515-528.

Wang, H., Qin, Q.H. and Kang, Y.L. (2005), A new meshless method for steady-state heat conduction problems in anisotropic and inhomogeneous media. *Arch Appl Mech*, 74, pp. 563-579.

Würkner M., Berger H., Gabbert U. (2011), On numerical evaluation of effective material properties for composite structures with rhombic fiber arrangements. *Int J Eng Sci*, 49, pp. 322-332.

Yang, Q.S. and Qin, Q.H. (2003), Modelling the effective elasto-plastic properties of unidirectional composites reinforced by fibre bundles under transverse tension and shear loading. *Mat Sci Eng A-Struct*, 344, pp.140-145.

Yang, Q.S. and Qin, Q.H. (2004), Micro-mechanical analysis of composite materials by BEM. *Eng Anal Bound Elem*, 28, pp. 919-926.

Yu, S.W. and Qin, Q.H. (1996), Damage analysis of thermopiezoelectric properties: Part II. Effective crack model. *Theor Appl Fract Mech*, 25, pp. 279-288.